Original Article

Accuracy of radiographic measurements of fracture-induced deformity in the distal radius

Acta Radiologica Open
12(9) 1–9

DOI: 10.1177/20584601231205986
journals.sagepub.com/home/arr
Sage

Janni Jensen[1,2], Ole Graumann[1,2], Oke Gerke[3,4], Trine Torfing[2], Helle Precht[5,6,7], Benjamin S Rasmussen[1,2,8] and Hans B Tromborg[4,9]

Abstract

Background: Management of the distal radius fracture (DRF) is to some extent based on radiographic characterization of fracture displacement. It remains unclear, however, if the measurements used to quantify displacement are accurate.

Purpose: To quantify accuracy of two radiographic measurements: dorsal/volar tilt and fracture compression, measured indirectly as ulnar variance (UV), using radiostereometric analyses (RSA) as reference standard.

Material and Methods: Twenty-one fresh frozen non-fractured human cadaveric forearms (right = 11, left = 10) were thawed and eligible for inclusion. The forearms were mounted on a custom made platform that allowed for controlled forearm rotation, and they underwent two rounds of imaging (both rounds consisted of RSA and radiographs). In round one, the non-fractured forearms were radiographed. In round two, artificial DRF´s with compression and dorsal angulation were created and imaging procedures repeated. Change in tilt and UV between the non-fractured and later fractured forearms was defined as fracture-induced deformity. Deformity was measured radiographically and additionally calculated using RSA. Bland Altman analyses were used to estimate agreement between radiographically measured, and RSA calculated, fracture-induced deformity.

Results: Our results indicated that radiographs underestimate the amount of fracture-induced deformity. Mean measured differences (bias) in dorsal tilt deformity between radiographs and RSA were −2.5° for both observers. The corresponding values for UV were −1.4 mm and −1.5 mm.

Conclusion: Quantifying fracture-induced deformity on radiographs underestimated the actual deformity when compared to RSA calculated deformity. These findings suggest that clinicians, at least in part, base fracture management and potentially corrective surgery on inaccurate measurements.

[1]Department of Radiology, Odense University Hospital, Odense, Denmark
[2]Research and Innovation Unit of Radiology, University of Southern Denmark, Odense, Denmark
[3]Department of Nuclear Medicine, Odense University Hospital, Odense, Denmark
[4]Department of Clinical Research, University of Southern Denmark, Odense, Denmark
[5]Health Sciences Research Centre, UCL University College, Odense, Denmark
[6]Department of Radiology, Kolding, Lillebaelt Hospital, University Hospitals of Southern, Kolding, Denmark
[7]Department of Regional Health Research, University of Southern Denmark, Odense, Denmark
[8]CAI-X (Centre for Clinical Artificial Intelligence), University of Southern, Odense, Denmark
[9]Department of Orthopedic Surgery, Odense University Hospital, Odense, Denmark

Corresponding author:
Janni Jensen, Research and Innovation Unit of Radiology, University of Southern Denmark, Kloevervaenget 10, Entrance 112, 2nd Floor, Odense C 5000, Denmark.
Email: janni.jensen@rsyd.dk

Keywords
distal radius fracture, measurements accuracy, dorsal tilt, radial inclination, ulnar variance

Received 15 May 2023; accepted 20 September 2023

Introduction

The distal radius fracture (DRF) is one of the most common types of orthopedic injuries, and the incidence appears to be increasing, particularly in the elderly population.[1] Traditionally, diagnosis and treatment of a DRF is partly based on radiographic characterization and quantification of fracture displacement. Computed tomography (CT) is primarily used as a supplementary diagnostic tool in equivocal cases, particularly to obtain detailed information on intra-articular involvement of the distal radius and/or the distal radioulnar joint.[2–4] Therefore, initial choice of treatment is often based on radiographs which is also reflected in numerous clinical practice guidelines (CPG) internationally. Although not identical, many CPG recommend including the radiographic measurements of dorsal tilt and ulnar variance (UV) in the treatment decision with suggested benchmark values above which fracture reduction or surgery is recommended.[2,3,5–8] An inherent issue when adding clinical value to radiographic measurements is reliability, which, in the case of a DRF, may be influenced by factors such as observer variability, method of measurements, and positioning of the forearm.[9–12] Another, equally important, although less explored, aspect is measurement accuracy. Can the three-dimensional morphology of a DRF be accurately described from two-dimensional radiographs? A recent systematic review was not able to uncover conclusive evidence on accuracy of neither dorsal/palmar tilt nor UV.[13] Given the widespread use of radiographic measurements in the clinical decision-making process and as predictors of outcome in patients with a DRF, strikingly little data on measurement accuracy is available, perhaps because of the lack of an acceptable reference standard. In a laboratory setting, radiostereometric analyses (RSA) can be used to estimate a reference standard for fracture induced displacement by quantifying movement of the distal fragment.

Accuracy of the radiographically measured dorsal tilt and UV remains uncertain implying that clinical decision-making and management of DRFs may, in part, be based on uncertain measurements warranting further studies exploring this topic. Accordingly, we designed a cadaver study with the objectives of estimating accuracy of the radiographically measured fracture-induced deformities of dorsal tilt and UV using RSA as reference standard.

Material and methods

Ethical approval was waived by the Regional Ethics Committee in accordance with the Danish law of health §14, (Project-ID: S-20180077). This study was methodologically designed and data collected, analyzed, and reported with adherence to the Standards for Reporting of Diagnostic Accuracy Studies (STARD) statements.[14]

Preparation of specimens

Radiostereometric analysis is a research tool that can be used to calculate the exact position of two segments in three dimensions. The segments are point matrices defined by small tantalum markers inserted into the bone. Two radiographs are taken simultaneously through a calibration box, and by use of RSA software, positions in space of the segments are determined. Subsequently, movement of one segment relative to another segment, as seen in the case of a displaced fracture, is calculated and reported as translation and rotation.[15]

Twenty-one fresh frozen human cadaveric forearms, severed mid-humerus, were consecutively thawed and eligible for inclusion (11 right; 10 left). The arms were prepared for RSA analyses by insertion of markers in the form of spherical tantalum beads, sizes 0.8 and 1.0 mm into the non-fractured distal radii in two segments, a distal periarticular segment and a segment approximately 4–6 cm above the radio-carpal joint. Distance between the two marker-segments was made such that an artificial fracture could be created approximately midways between the segments at a later stage. In the first six forearms, the markers were injected into cancellous bone using a spring-loaded piston (RSA Biomedical AB, Umeaa, Sweden). In arms 7–21, the markers were placed in cortical bone in predrilled holes and secured with bone-wax. This change in marker insertion allowed for a more controlled placement of the markers. The non-fractured forearms with tantalum markers were attached to a custom-made radiolucent platform. The forearms were rigidly secured to a wooden base on the platform with one Kirschner-wire (K-wire) from the distal humerus through the olecranon and 2–3 K-wires obliquely inserted from the ulna through the olecranon into the wooden base (Fig. 1). This set-up allowed the radius to rotate over a stationary ulna.

Image acquisition

To come as close to widely accepted radiographic positioning and imaging procedure, the following mounting and imaging techniques were applied. The forearms were positioned for a true lateral radiograph in neutral mid-prone

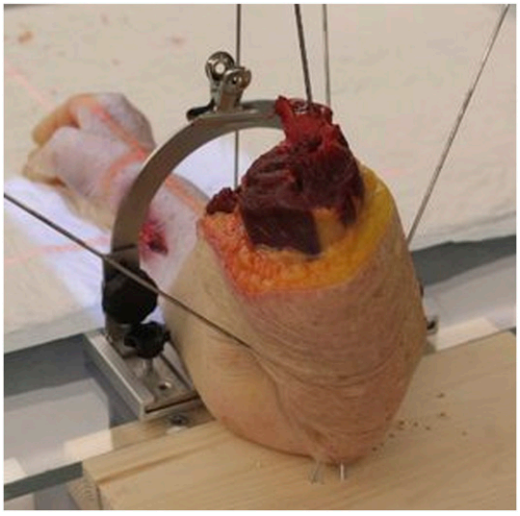

Figure 1. Forearm secured to wooden platform with K-wires through the distal portion of the forearm and the olecranon.

forearm rotation with the elbow flexed approximately 90° and the ulna towards the platform. Neutral rotation was defined as a radiograph where the most palmar aspect of the pisiform superimposed the central third of the interval between the palmar aspects of the capitate and the scaphoid.[16]

A slot underneath the platform allowed for the detector to be placed under the forearm for the lateral radiograph. For the cross-table posterior-anterior (PA) radiograph, the detector was positioned beside the table resulting in an object-to-detector distance. Hence, a calibration ball of known size was positioned above the wrist and UV measurements corrected accordingly. The platform was positioned such that the longitudinal axis of the forearm was parallel to the y-axis of the RSA calibration cage (uniplanar cage 43, RSA Biomedical AB, Umeaa, Sweden).

A mobile x-ray unit connected to a ceiling mounted tube allowed for synchronized acquisition of RSA images (MultitomRax and MiraMax1, Siemens Healtineers, Forchheim Germany). The RSA images were made with 140 cm focus-to-detector distance and tubes angled 17° relative to the calibration cage. The ceiling mounted tube was used for acquisition of radiographs at a focus-to-detector distance of 100 cm. The radiographs were taken with the center of the x-ray beam directed at the radial styloid. The PA and lateral radiographs were acquired at 50 kVp and 2.5 mAs and the RSA images at 89 kVp and 14 mAs.

Seven sets of RSA images and radiographs (PA and lateral) were taken of each forearm beginning with the non-rotated image with the forearm in mid-prone position. In order to mimic the variability in positioning occasionally seen in clinical practice, where true PA and lateral radiographs are not always possible, the procedure was repeated with the donor-arms slightly rotated, that is, supinated and pronated. Using a K-wire in the proximal radius against a goniometer attached to the platform, the procedure was repeated with the donor-arms rotated in increments of an estimated 5° (−15°, −10°, −5°, 0°, +5°, +10°, +15°). Negative values indicate supination and positive values pronation. As a result, three pronated, one neutrally positioned, and three supinated radiographs and RSA stereographs were obtained of each arm. Radiographs and RSA images were obtained in the same position before rotating to the next position.

Creation of fracture

Following completion of round one (non-fractured images), the forearms were detached from the platform, and a consultant hand surgeon created artificial DRFs with compression and dorsal angulation. The fractures were created approximately midways between the two marker segments. The radius was accessed via a dorsal approach. Using a K-wire drill the radius was weakened and an osteotome was used to further break the cortical bone. During the procedure, attempts were made to protect soft tissue including ligaments. The distal fragment, containing the periarticular distal marker segment, was manually displaced in a proximal and dorsal direction. It was attempted to induce approximately 10° of dorsal tilt, which is the degree of displacement commonly suggested for surgical decision making in CPGs.[2,6] Hereafter, the fracture was stabilized using crossed K-wire fixation. Two to three K-wires were introduced in the distal-proximal direction through the fracture site. If additional control of the distal fragment was deemed necessary, another K-wire was inserted. It was attempted to avoid projection of K-wires over anatomical landmarks used for radiographic measurements. Finally, the forearms were re-attached to the platform and the RSA and radiographic procedures were repeated as described above. Hence, all forearms underwent two rounds of RSA and radiographic imaging, that is, non-fractured, and fractured.

Fracture-induced deformity

Fracture-induced deformity was defined as the change in tilt and UV brought on by creation of fracture, that is, the relative difference between radiographic measurements from the non-fractured to the later fractured forearm.

Radiographs

Radiographs were stored in a Picture Archiving and Communication System (GE healthcare, Illinois, USA). Two observers with more than 20 years of experience, namely a musculoskeletal radiologist (“Blinded for anonymity”) and a consultant hand surgeon (“Blinded for

Figure 2. Radiographic measurements. Ulnar variance is measured as the difference i axial length between two lines perpendicular to the longitudinal axes of the radius. The two lines are placed against the most distal points of the ulnar and radial articular surfaces, respectively. Dorsal/volar tilt of the radial articular surface is measurend as the angle between two lines, one line connecting the palmar and dorsal surfaces of the distal radius and a line perpendicular to the longitudinal axes of the radius.

anonymity"), independently measured dorsal tilt and UV in a blinded and randomized fashion. A detailed protocol on measuring technique was presented to the observers to maximize consistency. Tilt was defined as angulation of the radial articular surface in the coronal plane. Ulnar variance, the length of the ulna relative to the radius, was used as an indirect expression of axial fracture compression or diastases (Fig. 2). Observers entered the measurements into an electronic database (REDCap, Research Electronic Data Capture).

RSA

For the purpose of this study, the RSA calculated magnitudes of fracture deformity were defined as reference standard. By comparing change in positioning of the distal segment in the fractured forearm relative to the same forearm prior to creation of fracture, quantification of RSA calculated fracture-induced deformity was achieved. The forearms were positioned in a lateral position along the y-axis of the calibration cage. Hence, according to the RSA coordinate system, rotation of the distal segment around the Z-axis (Z^r) was an expression of dorsal tilt (negative values) and palmar tilt (positive values). Fracture compression was comparable to positive translation of the distal fragment along the Y-axis (Y^t) where negative values would indicate fracture diastasis. Signed values for tilt were reverted for left arms. All RSA analyses were made using the UmRSA software system (7.0, RSA Biomedical AB, Umeaa, Sweden) by one author (JJ).

Eligibility criteria

Individual tantalum marker segments were defined as rigid bodies. By comparing marker configuration between two or more exams, the rigid body model can be tested for

deviations indicating unstable markers. Movement of marker(s) within a segment was expressed as the mean error of rigid body (ME), and calculated by the RSA software. To minimize bias from unstable markers, an upper limit of ME ≤ 0.35 mm was used as eligibility criteria.[17] Additionally, the condition number, calculated by the RSA software was presented as an indication of marker dispersion within the arms. Low condition numbers indicate well-dispersed markers where close and/or co-aligned markers increase the condition number.[18] Condition numbers <300 is recommended.[19]

Statistical analyses

Radiographic and RSA fracture-induced deformities were presented as mean and standard deviation (SD). Spatial marker distribution as described by the condition number was presented as mean and range. Agreement between RSA and radiographically estimated fracture-induced deformity was assessed and illustrated using Bland–Altman (BA) plots with Limits of Agreement (LoA) and 95% confidence intervals (CI).[20,21] Results were considered statistically significant if $p < .05$. The Stata Version 16 (StataCorp. 2019, TX) was used for all statistical analyses.

Results

Three donor-arms were excluded based on an ME above 0.35. One donor arm had to be excluded as K-wires superimposed on tantalum markers to an extent where the RSA-analyses could not be made. A final cohort of 17 donor-arms, 8 right and 9 left, were included. With seven radiographs and RSA-images of each forearm, 119 sets of images were included from each round of imaging, that is, non-fractured and fractured. Condition numbers ranged from 34 to 311 (Table 1).

Table 1. Forearm condition numbers based on RSA analyses.

	Non-fractured	Fractured
	Mean (range)	Mean (range)
Proximal segment	146 (89 to 297)	144 (89 to 311)
Distal segment	55 (34 to 116)	50 (34 to 86)

Non-fractured (n = 147); Fractured (n = 119).

Table 2. Fracture induced deformity. Mean measured fracture induced deformities of observer 1, 2, and RSA, respectively, based on data from all radiographs (n = 119) and from the reference (non-rotated) radiographs (n = 17).

	Radiographs	Tilt Mean (SD)	Fracture compression Mean (SD)
Observer 1	All	14.3 (10.6)	0.2 (1.4)
	Reference	12.1 (10.2)	0.0 (1.2)
Observer 2	All	14.4 (9.2)	0.1 (1.6)
	Reference	12.7 (12.8)	0.3 (1.5)
RSA	All	16.9 (6.6)	1.6 (1.6)

All: All radiographs (supinated, pronated and non-rotated), Reference: Non-rotated reference radiographs, SD: Standard deviation; RSA: Radiostereometric analyses; Tilt reported in degrees and fracture compression in mm.

Accuracy of fracture induced deformities

Both observers agreed that the radiographically measured fracture induced deformity of both dorsal tilt and UV was underestimated when compared to the deformity calculated using RSA. When including images in all degrees of forearm rotation, the mean radiographically measured change in tilt brought on by fracture was 14.3° (SD = 10.6) and 14.4° (SD = 9.2) for observer 1 and 2, respectively (Table 2). Including only measurements from the non-rotated images, the values were 12.1° (SD = 10.2) and 12.7° (SD = 12.8) for observer 1 and 2, respectively. The corresponding value was 16.9° when calculated by RSA, indicating that radiographically measured tilt is underestimated with between 2 and 4°. Radiographically measured fracture-induced deformity of compression was underestimated by 1.4 and 1.5 mm for observer 1 and 2, respectively, in comparison to RSA calculated fracture compression.

Using the BA LoA analyses, the bias estimates between radiographic and RSA calculated fracture-induced displacement were all negative and statistically different from 0, thus they supported the notion that the radiographic measurements underestimate fracture displacement. Mean measured difference between radiographs and RSA of fracture induced tilt was −2.5° (95% CI: −4.23 to −0.82) and −2.5° (95% CI: −3.9 to −1.1) for observer 1 and 2, respectively (Table 3). Disagreement between radiographs and RSA is further emphasized by broad LoA. The outer BA LoA (dorsal tilt) for observer 1 and observer 2 versus RSA were −23.66 to 18.62 and −19.67 to 14.73, respectively. Bias for fracture compression were −1.4 mm (95% CI: −1.64 to −1.14) and −1.5 mm (95% CI: −1.79 to −1.16) for observer 1 and 2, respectively. Bland–Altman plots with LoA, bias and respective 95% CI are shown for RSA versus observer 1 and 2 for tilt and fracture compression, respectively, in Fig. 3.

Discussion

Despite the fact that RSA is not a clinical tool available for measuring tilt and UV in patients with a DRF, the results from the current study does suggest the need for a critical evaluation of methods in regard to radiographic

Table 3. Bland–Altman limits of agreement and mean estimated differences between RSA and observer 1 and 2, respectively.

		Bias Mean (SD)	Bias 95% CI	Limits of agreement	95% CI of lower limit of agreement	95% CI of upper limit of agreement
Tilt	O_1 vs. RSA	−2.5 (9.4)	−4.23 to −0.82	−20.89 to 15.83	−23.66 to −18.87	13.82 to 18.62
	O_2 vs. RSA	−2.5 (7.7)	−3.90 to −1.10	−17.41 to 12.46	−19.67 to −15.77	10.83 to 14.73
Fracture	O_1 vs. RSA	−1.4 (1.4)	−1.64 to −1.14	−4.12 to 1.34	−4.54 to −3.82	1.04 to 1.75
Compression	O_2 vs. RSA	−1.5 (1.7)	−1.79 to −1.16	−4.74 to 1.83	−5.24 to −4.38	1.47 to 2.32

SD: Standard deviation; CI: confidence interval; O_1: observer 1; O_2: observer 2; RSA: Radiostereometric analyses; Tilt is reported in degrees; Tilt, Dorsal (−), Palmar (+); Fracture compression is in mm.

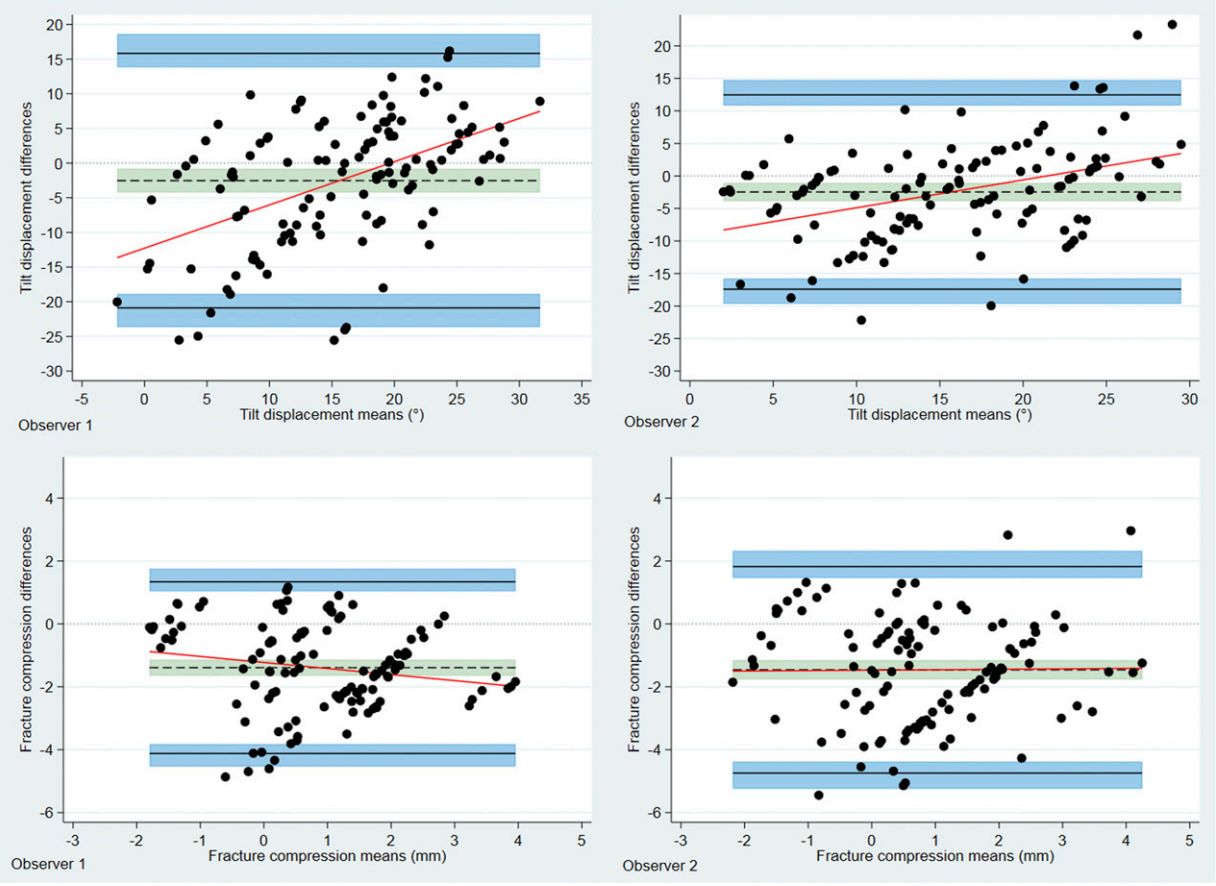

Figure 3. Bland-Altman plots displaying differences between RSA and radiographically measured fracture induced deformity for both observers. Differences are found by deducting the RSA value from the radiographically measured value. The solid black lines indicate upper and lower 95% limits of agreement, shaded blue areas depict respective confidence intervals. The dotted line represents the estimated bias, that is, the mean measured difference between RSA and radiographs; shaded green areas show respective confidence intervals. The bias line is below zero in all cases, indicating that radiographic measurements underestimated the measured values when compared to RSA.

characterization of DRFs, including the radiographic procedure and method of measurement.

In the current study, the radiographically measured fracture-induced deformities of dorsal tilt and fracture compression were systematically underestimated when compared to the RSA calculated fracture deformity. Contrastingly, it was previously reported that fracture deformity of tilt was overestimated when measured in radiographs.

Computed tomography (CT) bone-surface models were used as reference standard and fracture-induced deformity defined as the difference between fractured and contralateral unaffected forearm.[22,23] The use of contralateral forearm could potentially explain that outcomes were contradictory to those reported in the current study. The laboratory nature of our study allowed for the same arm to serve as its own control, before and after creation of fracture, minimizing bias in regard to possible morphological variation in between contralateral limbs. Another explanation could be that anatomical landmarks may be differently depicted and identified in three-dimensional bone models as compared to two-dimensional radiographs. The finding that RSA and CT demonstrate opposing results warrants additional research though, particularly since CT may be used in cases that are more complex where the radiographic characterization of fracture is deemed insufficient.

In keeping with our findings, however, both aforementioned studies reported that UV, as an expression of fracture compression, was underestimated on radiographs.[22,23] The three-dimensional multiplanar deformity typically displayed in a DRF may, possibly be the primary contributor to the finding that fracture compression is underestimated when measured radiographically. It has previously been suggested that dorsal angulation introduce bias to UV measurements made in the coronal plane.[24] Anatomically, the dorsal aspect of the distal radius extends distally in comparison to the palmar aspect, forming the normal palmar tilt of approximately 12° in the sagittal plane.[25] In the current study, the palmar cortical rim of the sigmoid notch was used when measuring UV. Dorsal angulation of the distal fragment may, however, displace the palmar aspect of the radial articular surface distally when seen in the PA radiograph. If the ***palmar*** aspect of the radial articular surface is displaced distally, the measurement of fracture compression may be underestimated when measured as the relative difference in axial length between the fractured radius and the unaffected ulna. This notion is supported by Athlani and colleagues who found that fracture compression was underestimated less in a group of DRF patients displaying palmar deformity than in a group with dorsal deformity.[23]

Moreover, it has been suggested that the radiographically depicted sclerotic demarcation of the ***palmar*** aspect of the sigmoid notch disappears in fractures with pronounced dorsal angulation and instead the ***dorsal*** aspect of the sigmoid notch is seen as the sclerotic demarcation.[26] If this holds true, two different landmarks may have been used to measure UV between the non-fractured and later fractured forearms in the current study. Clinically, this would indicate that two different anatomical landmarks may be used to quantify fracture compression before and after reduction of a compacted DRF fracture with dorsal angulation. Consequently, fracture compression, estimated indirectly using UV, should be interpreted with caution, particularly in the presence of pronounced dorsal angulation.

One could argue though, that the clinical relevance of a systematic underestimation of radiographic fracture deformity may be of little clinical significance given the fact that the thresholds suggested in CPGs are derived from radiographic measurements and not from CT or RSA. Therefore, a potential systematic underestimation is presumably indirectly incorporated into the guidelines. Consequently, if one universally accepted reliable method of measuring existed, the systematic underestimation of radiographic measurements suggested in the current study would perhaps not be of clinical importance. There are, however, different techniques described for measuring UV and if accuracy and or reliability varies in between those methods, it becomes problematic to establish reliable benchmark values for treatment and outcome.[27,28]

A key aspect of an accuracy study is the availability of a valid reference standard. Literature on accuracy of radiographic wrist measurements is sparse, most likely because of the lack of a reference standard that reflects the truth adequately. The use of RSA as reference standard is a limitation in the sense that the exact methodology applied in the current study has not been used previously. RSA has been shown to calculate micro-motion of DRF´s with high precision and accuracy though.[29] Marker based RSA calculates movement based on geometric polygons made up of patient markers. The anatomical region within which these markers are dispersed does not influence analyses of movement. We therefore presume that RSA was a valid tool when calculating fracture induced deformities in the current study. The use of a cadaveric model is a limitation, which may compromise generalizability to an in vivo clinical setting. While rigor mortis was not present after defrosting the forearms, we cannot rule out the possibility of ligament laxity, which might have influenced the distal radio-ulnar relationship during forearm rotation.

In conclusion, this study demonstrated the difficulty of accurately measuring displacement of a DRF on radiographs. When using the RSA calculated fracture-induced deformity as reference standard, all corresponding radiographic measurements underestimated the fracture-induced deformities. As such, the most accurate and reliable method when quantifying tilt and UV remains unclear. Further research is needed to improve our understanding of how to most accurately and reliably quantify displacement in a DRF and explore the difference between the various methods of measuring.

Author contributions

All authors have read and approved the final submitted manuscript.

Declaration of conflicting interests

The author(s) declared no potential conflicts of interest with respect to the research, authorship, and/or publication of this article.

Funding

The author(s) disclosed receipt of the following financial support for the research, authorship, and/or publication of this article: This work was supported by the Grosser A V Lykfeldt and wife fund, the Grosserer L. F. Foghts Fund, RadiografRådet, and Torben og Alice Frimodts Fond. The funding bodies had no influence on study design, data collection, and analyses or the publication process.

ORCID iDs

Janni Jensen https://orcid.org/0000-0001-7036-6129
Ole Graumann https://orcid.org/0000-0002-9663-8361
Oke Gerke https://orcid.org/0000-0001-6335-3303

References

1. Kakar S, Noureldin M, Van Houten HK, et al. Trends in the incidence and treatment of distal radius fractures in the United States in privately insured and medicare advantage enrollees. Hand (NY) 2020; 17: 331–338.
2. Danish Department of Health. National clinical guideline on the treatment of distal radial fractures. Available at: https://www.sst.dk/-/media/Udgivelser/2014/NKR-H%C3%A5ndledsn%C3%A6re-underarmsbrud/National-clinical-guideline-on-the-treatment-of-distal-radial-fractures.ashx?sc_lang=da&hash=A867AD76B6ECFF5A7307A0C006E0938A (2022, accessed 25 March 2022).
3. Treatment of distal radius fractures in adults - Norwegian orthopaedic association - The Norwegian medical association. Available at: https://files.magicapp.org/guideline/ac10868f-c18b-462d-978d-cb53a5959fd5/2_6/pdf/published_guideline_551-2_6.pdf (2023, accessed 6 May 2023).
4. Katz MA, Beredjiklian PK, Bozentka DJ, et al. Computed tomography scanning of intra-articular distal radius fractures: does it influence treatment? J Hand Surg AM 2001; 26: 415–421.
5. Värttinäluun alaosan murtuma (rannemurtuma). Available at: https://www.kaypahoito.fi/hoi50109 (2022, Accessed 25 March 2022).
6. Lichtman DM, Bindra RR, Boyer MI, et al. American Academy of Orthopaedic Surgeons clinical practice guideline on: the treatment of distal radius fractures. J Bone Joint Surg Am 2011; 93: 775–778.
7. British Orthopaedic Association and British Society for Surgery of the Hand. Best practice for management of Distal Radial Fractures (DRFs). Available at: https://www.bssh.ac.uk/_userfiles/pages/files/professionals/Radius/Blue_Book_DRF_Final_Document.pdf (2023, accessed 6 May 2023).
8. Die Deutsche Gesellschaft für Unfallchirurgie. Leitlinie distale radiusfraktur des erwachsenen. Available at: https://register.awmf.org/assets/guidelines/012-015l_S2e_Distale_Radiusfraktur_2021-11_02.pdf (2023, accessed 6 May 2023).
9. Capo JT, Accousti K, Jacob G, et al. The effect of rotational malalignment on X-rays of the wrist. J Hand Surg Eur 2009; 34: 166–172.
10. Jensen J, Tromborg HB, Rasmussen BSB, et al. The effect of forearm rotation on radiographic measurements of the wrist: an experimental study using radiostereometric analyses on cadavers. Eur Radiol Exp 2021; 5(5): 15.
11. Jensen J, Tromborg HB, Rasmussen BSB, et al. Dorsal tilt of the distal radius fracture changes with forearm rotation when measured on radiographs. Journal of HandSurgery Global Online 2021; 3(4): 182–189.
12. Pennock AT, Phillips CS, Matzon JL, et al. The effects of forearm rotation on three wrist measurements: radial inclination, radial height and palmar tilt. Hand Surg 2005; 10: 17–22.
13. Jensen J, Rasmussen BS, Duus LA, et al. Distal radius fractures and radiographic assessment: a systematic review of measurement accuracy. Acta radiologica (Stockholm, Sweden : 1987) 2019; 60(11): 1482–1489.
14. Cohen JF, Korevaar DA, Altman DG, et al. STARD 2015 guidelines for reporting diagnostic accuracy studies: explanation and elaboration. BMJ Open 2016; 6: e012799.
15. Selvik G. Roentgen stereophotogrammetry. A method for the study of the kinematics of the skeletal system. Acta Orthop Scand Suppl 1989; 232: 1–51.
16. Yang Z, Mann FA, Gilula LA, et al. Scaphopisocapitate alignment: criterion to establish a neutral lateral view of the wrist. Radiology 1997; 205: 865–869.
17. Valstar ER, Gill R, Ryd L, et al. Guidelines for standardization of radiostereometry (RSA) of implants. Acta Orthop 2005; 76: 563–572.
18. Holm-Glad T, Reigstad O, Tsukanaka M, et al. High precision and accuracy of model-based RSA for analysis of wrist arthroplasty. J Orthop 2018; 36: 3053–3063.
19. Downing MR, Ashcroft PB, Johnstone AJ, et al. Assessment of inducible fracture micromotion in distal radial fractures using radiostereometry. J Orthop Trauma 2008; 22: 96–105.
20. Bland JM, Altman DG. Measuring agreement in method comparison studies. Stat Methods Med Res 1999; 8: 135–160.
21. Gerke O. Reporting standards for a Bland-Altman agreement analysis: A review of methodological reviews. Diagnostics (Basel) 2020; 10(5)–160.
22. Miyake J, Murase T, Yamanaka Y, et al. Comparison of three dimensional and radiographic measurements in the analysis of distal radius malunion. J Hand Surg Eur 2013; 38: 133–143.
23. Athlani L, Chenel A, Berton P, et al. Three-dimensional versus radiographic measurements for analyzing extra-articular distal radius malunion. J Hand Surg AM 2020; 45: 984.e1–984.e7.
24. Haus BM, Jupiter JB. Intra-articular fractures of the distal end of the radius in young adults: reexamined as evidence-based and outcomes medicine. J Bone Joint Surg Am 2009; 91: 2984–2991.

25. Namazi H, Khaje R. Normal age-related alterations on distal radius radiography. Arch Bone Jt Surg 2015; 3: 250–253.
26. Medoff RJ. Essential radiographic evaluation for distal radius fractures. Hand Clin 2005; 21: 279–288.
27. Steyers CM, Blair WF. Measuring ulnar variance: a comparison of techniques. J Hand Surg AM 1989; 14: 607–612.
28. Bernstein DT, Linnell JD, Petersen NJ, et al. Correlation of the lateral wrist radiograph to ulnar variance: a cadaveric study. J Hand Surg AM 2018; 43: 951.e1–951.e9.
29. Madanat R, Makinen TJ, Moritz N, et al. Accuracy and precision of radiostereometric analysis in the measurement of three-dimensional micromotion in a fracture model of the distal radius. J Orthop Res 2005; 23: 481–488.